

# Separable Four Points Fundamental Matrix

Gil Ben-Artzi

Ariel University, Ariel, Israel  
gilba@ariel.ac.il

**Abstract.** We present an approach for the computation of the fundamental matrix based on epipolar homography decomposition. We analyze the geometrical meaning of the decomposition-based representation and show that it guarantees a minimal number of RANSAC samples, on the condition that four correspondences are on an image line. Experiments on real-world image pairs show that our approach successfully recovers such four correspondences, provides accurate results and requires a very small number of RANSAC iterations.

**Keywords:** Fundamental Matrix, Epipolar Geometry, 3D reconstruction, RANSAC

## 1 Introduction

One of the basic building blocks in computer vision is the computation of epipolar geometry given a set of putative image point correspondences. Often, such correspondences include mismatches, therefore a robust estimation method is needed to be carried out. The most common method used is RANSAC [10]. RANSAC-based computation of the fundamental matrix iteratively samples a minimal set of putative points' correspondences, hypothesizes the fundamental matrix parameters and evaluates their goodness-of-fit with respect to the whole set of the putative points' correspondences. This process is repeated until a pre-defined number of iterations is exceeded. One of its key limitations is that in the presence of a considerable amount of mismatched points' correspondences, a large number of evaluations is needed in order to obtain a reliable model. Hereafter, when referring to iterations we refer to the number of evaluation iterations.

The number of the required iterations is directly related to the number of points needed to be sampled in order to hypothesize the fundamental matrix parameters. From a geometrical point of view, the minimal sample size is at least seven [12]. Minimal sample approaches have been proposed requiring only five or six points' correspondences [25,2]. They often require additional knowledge regarding the parameters and/or the presence of a special structure in the scene, such as a planar surface.

Here, we present an approach that can markedly reduce the number of RANSAC iterations for the computation of the fundamental matrix, both theoretically and practically. We require that four correspondences are on line segment in the images and show empirically that such configuration is common. We

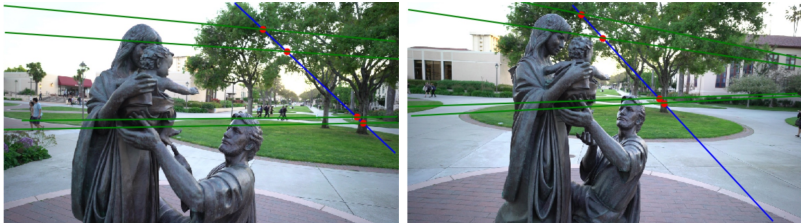


Fig. 1: Our approach match points on line segments in the images without the need for the full computation of the fundamental matrix. Based on the matched points and line segments, we use our reformulation to compute the epipolar homography and markedly reduce the required number of RANSAC iterations for the full computation. The red points are the matched putative correspondences which are aligned on line segments (blue lines) in the image planes. The green lines are epipolar lines which are not known a-priori and do not take part in the matching process. The matching process is based on the computation of the epipolar homography which, unlike commonly used methods, does not require the knowledge of epipolar line correspondences.

compute the fundamental matrix in two steps. In the first step, we sample three points on line segments. We compute the epipolar homography and validate its goodness of fit using at least one additional point, without the full computation of the fundamental matrix. In the second step, the recovered matches are fixed and the remaining points' matches are recovered by sampling, without any restriction. The sampled points in the first step are not necessarily related by a physical 3D line in the captured scene. Figure 1 shows four such matches. The red points are corresponding points that are on line segments in the images. The green lines are epipolar lines. Methods based on the computation of the epipolar homography [14,24,6,11,12] are rarely used in practice, due to the requirement for the knowledge of (at least) three corresponding epipolar lines. We show here how to compute the epipolar homography without a-priori knowledge of epipolar lines. Fig. 2 shows the required number of RANSAC iterations for the computation of the fundamental matrix, by our approach and existing minimal methods, as a function of the outlier rate. The minimal method of [2] requires a planar surface on the scene and we require four correspondences on a line segment in the images. We compared two cases. In the ideal case, the number of RANSAC iterations is based on only one solution per sample. In the practical case, we also take into account the number of solutions in the seven-points based algorithm which can be between one and three and our preprocessing iterations. In both cases our approach presents the minimal number of required iterations.

This paper therefore contributes by presenting: (a) a reformulation of the fundamental matrix based on epipolar homography decomposition and an analysis of its geometrical meaning, (b) a novel two steps RANSAC based approach for the computation of the fundamental matrix and (c) a validation of our ap-

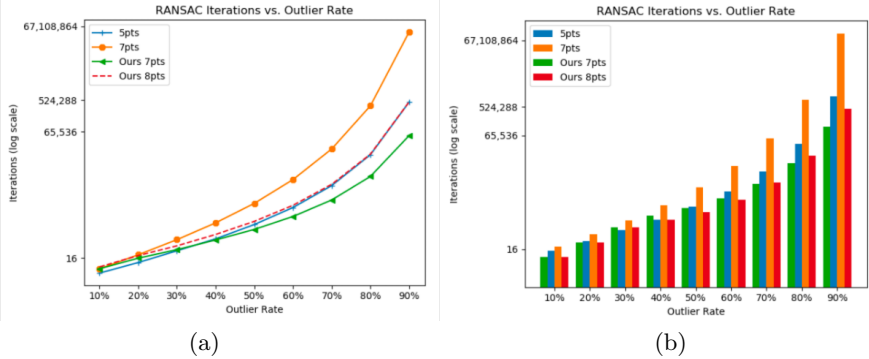


Fig. 2: The required number of RANSAC iterations for the computation of the Fundamental matrix. 5pts is the state-of-the-art minimal method of [2] and 7pts is the 7-points algorithm. Ours 7pts (8pts) represents our approach, using the seven (eight) points algorithm. In both figures, success probability of RANSAC is 0.99. (a) The expected theoretical number of RANSAC iterations, considering only one solution per iteration. (b) The expected practical number of RANSAC iterations. The computation includes the average number of evaluations required in practice by methods which use the 7-points based solution and the additional preprocessing iterations required by our approach. Based on our experiments, the number of solutions per sample is 2.43 and the average number of iterations for our preprocessing is 59 (See Sec. 6.4). In both cases, ideal and practical, our approach presents a new minimal number of RANSAC iterations for the computation of the Fundamental matrix.

proach on real-world image pairs showing that it is accurate and that it requires only a small number of RANSAC iterations.

## 2 Related Work

The most common approaches for the computation of the fundamental matrix are the seven or eight points algorithm [12]. The eight points algorithm [16] which was adapted for the fundamental matrix, was made practical by [13]. It is based on the normalization of the points' correspondences, and computes the parameters based on the Direct Linear Transform (DLT) by enforcing the rank 2 constraint [18]. The seven points algorithm relaxes the eight points requirement by an additional zero determinant constraint of the matrix, resulting in a cubic equation with one or three real solutions.

Various minimal methods assume additional knowledge in order to reduce the required number of correspondences. If the camera parameters are known, the five-points algorithm [19] can be used. Recently, Barath [2] proposed an approach for the estimation of the fundamental matrix based on five correspondences, in

case of three co-planar point correspondences and the rotation of features are known. Ben-Artzi et al. [5] showed that in case the intensity of the epipolar lines are similar across views, two corresponding points are sufficient for the computation of matching epipolar lines, and can be used for recovery of the fundamental matrix.

Methods attempting to empirically reduce the number of RANSAC iterations have also been introduced [4,7,20]. Unlike such methods, our approach, as well as other minimal methods, guarantees to reduce the number of required samples and this number can be calculated in advance in the same way as in standard RANSAC. In addition, our approach has a true geometrical meaning (See Sec. 3), whereas no geometrical analysis is possible in such methods.

The fundamental matrix can be computed based on the epipolar homography [12,9]. These methods require the knowledge of epipolar line correspondences. Sinha [24] introduced an approach for camera calibration based on the computation of the epipolar homography and epipoles hypothesizing. His approach was later improved by [6], who directly recovered the epipolar lines required for the computation of the epipolar homography by using the motion-barcode descriptor. Similar approaches were introduced by [14,11] for the computation of the epipolar homography by directly estimating the epipolar lines. However, all of the above methods are only applicable to videos of dynamic scenes. Wurfl et. al. [30] presented an approach for estimating the fundamental matrix transmission imaging, based on the epipolar homography formulation. They do not require explicit correspondences but rather sampling of all edge pixels of the image. The computation of the relative pose by general line homography based on line segments was demonstrated by [21] but they required the matching points to be the projection of existing 3D lines in the scene and required at least two such lines.

### 3 Theoretical Background

**Epipolar-Lines Based Parametrization.** Let  $l, l'$  be corresponding epipolar lines, in the first and second image, respectively. Let  $l_p$  be a line that intersects  $l$  in the point  $p$  and does not include the epipole. It follows that  $p = l_p \times l$ , where  $\times$  is the cross product. Since  $p$  is on  $l$ , it follows that  $l' = Fp$ . Denote  $[\cdot]_x$  as the skew symmetric matrix associated with the cross product, we have the following mapping:

$$l' = F[l_p]_x l$$

where  $H_l = F[l_p]_x$  is the epipolar homography. The seven degrees of freedom of the fundamental matrix is constructed by the four degrees of freedom of the two epipoles and the three degrees of freedom of the epipolar homography [12]. The epipolar homography is obtained by three corresponding epipolar lines.

**Image-Points' Based Parametrization.** Consider the set of epipolar lines passing through the epipole which is denoted as the *pencil of epipolar lines*. As shown in Fig. 3, the corresponding epipolar lines across images define a

plane which intersects the two retinal planes with its axis as the baseline. When the corresponding epipolar lines rotate around the epipoles, their corresponding planes rotate around the baseline, defining the *pencil of epipolar planes*. The two corresponding pencils of epipolar lines are related by the epipolar homography based on the pencil of epipolar planes [9]. Let  $(l_i, l'_i)$  be corresponding epipolar lines in the first and second image respectively. Let  $\bar{l}, \bar{l}'$  be arbitrary lines in the first and second image, such that the epipoles  $e, e'$  are not on the lines. The  $2 \times 2$  epipolar homography  $H_e$  maps between  $(l_i, l'_i)$  based on their intersection *points* with  $\bar{l}, \bar{l}'$  as follows. Let  $x_1, x_2 \in \bar{l}$  and  $x'_1, x'_2 \in \bar{l}'$ , denoted as *control points*. The intersection points of  $(l_i, l'_i)$  with  $\bar{l}, \bar{l}'$  are  $x_p = (x_1 \times x_2) \times l_i$  and  $x_{p'} = (x'_1 \times x'_2) \times l'_i$ , where  $\times$  is the cross product and using homogeneous coordinates of the control points from now on. Using the following identity

$$v \times (u \times w) = (v^T w)u + (-v^T u)w$$

for  $u, v, w \in \mathbb{R}^{3 \times 1}$ , the intersection points can be written as a linear combination of the control points as  $x_p = \alpha x_1 + \beta x_2$  and  $x_{p'} = \alpha' x'_1 + \beta' x'_2$ , where

$$\alpha = l_i^T x_2, \quad \beta = -l_i^T x_1, \quad \alpha' = l'^T_i x'_2, \quad \beta' = -l'^T_i x'_1,$$

$\alpha, \beta, \alpha', \beta' \in R$ . The  $2 \times 2$  epipolar homography is given by:

$$\begin{bmatrix} \alpha' \\ \beta' \end{bmatrix} = \underbrace{\begin{bmatrix} a & b \\ c & d \end{bmatrix}}_{H_e} \begin{bmatrix} \alpha \\ \beta \end{bmatrix} \quad (1)$$

Rewriting the corresponding epipolar lines as the cross product of the epipoles and points on the epipolar lines, and expanding the intersection points' coefficients, we have the following parametrization of the fundamental matrix:

$$F \approx [e_2]_{\times} [x'_1, x'_2] \begin{bmatrix} a & b \\ c & d \end{bmatrix} \begin{bmatrix} x_2^T \\ -x_1^T \end{bmatrix} [e_1]_{\times} \quad (2)$$

**Observation 1.** The epipolar homography  $H_e$  maps between the corresponding points  $x_p, x'_{p'}$  based on their representation as a linear combination of their respective control points. It can be computed without the knowledge of the corresponding epipolar lines. Given the line segments of the points, we select (fixed) control points on the lines and represent the points as their linear combination. The points' based parametrization of the pencil of epipolar lines by their intersection with the lines  $\bar{l}, \bar{l}'$  is shown in Fig. 3.

**Observation 2.** The required number of RANSAC iterations for the full computation of the fundamental matrix can be greatly reduced. First, we recover

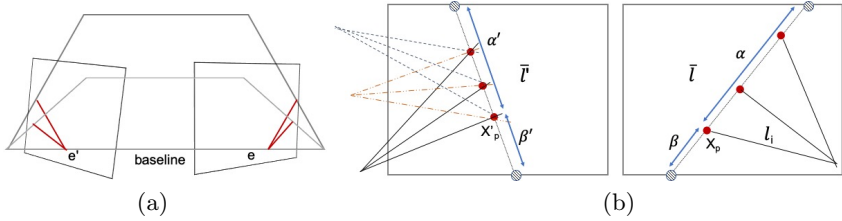


Fig. 3: (a) The pencil of epipolar planes. As the epipolar lines (red lines) rotate around the epipoles ( $e, e'$ ), their associated planes rotate around the baseline. (b) The epipolar homography has three degrees of freedoms, and each given pair of intersecting lines is the same regardless of the epipoles positions. On the left image, various epipole positions are valid for the same epipolar homography. Existing methods compute the epipolar homography based on epipolar lines. We show the points' based parametrization which enables the epipolar homography's computation regardless of the epipole positions. The parametrization of the intersection point  $x_p$  of the epipolar line  $l_i$  is based on a linear combination  $\alpha, \beta$  of selected fixed points on the lines, marked by the striped points, intersecting the boundaries of the image.  $x'_p$  is the corresponding intersection point of  $x_p$  and is parametrized by  $\bar{l}', \alpha', \beta'$ . See text for details.

$H_e$  which is a three parameters model without the need for the full computation of the fundamental matrix. We can then recover additional four arbitrary correspondences by relying on the recovered  $H_e$ . Let  $F(k, r)$  be the required number of RANSAC iterations for a model with  $k$  parameters, outlier rate  $r$  and success probability of 0.99. The required number of RANSAC iterations is now  $F(3, r) + F(4, r)$  instead of  $F(7, r)$ . The actual required number of iterations can be seen in Fig. 2.

**Observation 3.** The lines  $\bar{l}, \bar{l}'$  with the corresponding points are arbitrary line segments in the images. Figure 4 illustrates the mapping of points in the first image to lines in the second image, based on the parametrization of the fundamental matrix using the points' based epipolar homography (Eq. 2), given  $\bar{l}, \bar{l}'$ .

## 4 Line Segments with Corresponding Points

Our goal is to find the lines  $\bar{l}, \bar{l}'$  across images with the maximum number of putative points' correspondences. For each image, our approach does not require the knowledge of the points and lines in the other image, which allows concurrent implementation. The key idea is to use Hough transform [8] to detect the lines independently in each image and update a joint accumulator which can be queried only after the process is completed. Fig. 5 illustrates the matching process of corresponding lines across images.

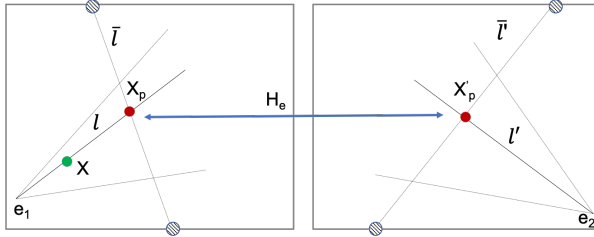


Fig. 4: The mapping of a point on the left image to the corresponding epipolar line on the right image by the fundamental matrix, parametrized by points-based epipolar homography  $H_e$ : (a) from a point  $x$  to epipolar line  $l$  based on the known epipole  $e_1$ , (b) from the epipolar line  $l$  to the intersection point  $x_p$  with a fixed arbitrary image line  $\bar{l}$ , (c) from the intersection point  $x_p$  to the corresponding intersection point  $x'_p$  with a fixed arbitrary line  $\bar{l}'$  and (d) from the point of intersection  $x'_p$  to the epipolar line  $l'$  based on the known epipole  $e_2$ .

Let  $I_1, I_2$  denote a pair of images. Let  $X = \{(x_i, x'_i)\}_{i=1..N}$  denote the set of ordered pairs of unique *putative corresponding image points* where  $x_i, x'_i \in \mathbb{R}^2$  are image points in  $I_1, I_2$ , respectively. Let  $\bar{X} = \{x_i\}_{i=1}^N$ ,  $\bar{X}' = \{x'_i\}_{i=1}^N$ . We create binary images  $B_1, B_2$  such that for each pixel  $y_i$  in  $I_1$ ,  $B_1(y_i) = 1$  if  $y_i \in \bar{X}$  otherwise  $B_1(y_i) = 0$ , and similarly for  $B_2$ . We use Hough transform [8] to extract the ordered set of lines  $L_1 = \{l_i\}_{i=1}^{K_1}$ ,  $L_2 = \{l'_i\}_{i=1}^{K_2}$  in  $B_1, B_2$ , respectively. We consider only lines with at least four correspondences. This requirement is due to the robust estimation process of the homography (See Sec. 5), where we sample three points and need at least one additional point to estimate the quality of the hypothesized homography.

We define a multidimensional array, an accumulator  $A$  of size  $N \times K_1 \times K_2$ , where  $K_1$  and  $K_2$  are the number of lines in  $L_1$  and  $L_2$ , respectively, and  $N$  is the number of putative corresponding points. The accumulator is initialized to zero. Let  $D_1(j) \subset \{1...K_1\}$  be the indices of nearby lines in  $L_1$  for a point  $x_j$  in image  $I_1$ ,

$$D_1(j) = \{i | l_i \in L_1, x_j \in \bar{X}, d(x_j, l_i) < C\}, \quad (3)$$

where  $d$  is the point to line distance and  $C$  is the constant representing the required distance between the lines and points. For each point  $x_j$  in the first image, we increment the accumulator according to its nearby lines in the first image and all existing lines in the second image,  $A(j, m, n) + 1$  s.t.

$$\{(j, m, n) | m \in D_1(j), n \in \{1...K_2\}\}, \quad (4)$$

For each point  $x'_j$  in the second image,  $D_2(j) \subset \{1...K_2\}$  is defined similarly and the accumulator entries  $(j, m, n)$  are incremented according to

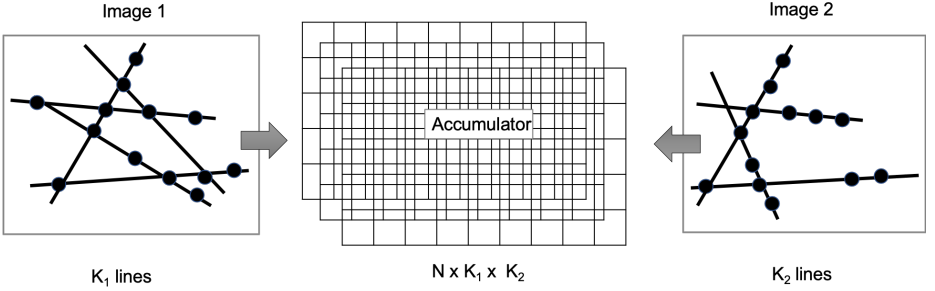


Fig. 5: We match points on line segments without the need to explicitly compare between lines across images. In each image, Hough transform is carried out and a shared accumulator of size  $N \times K_1 \times K_2$  is updated independently, where  $N$  is the number of correspondences,  $K_1$  is the number of lines in the first image and  $K_2$  is the number of lines in the second image.

$$\{(j, m, n) | m \in \{1 \dots K_1\}, n \in D_2(j)\}, \quad (5)$$

The pair of matching lines with the maximum number of putative points' correspondences are given by  $(l_{\mathbf{m}^*}, l'_{\mathbf{n}^*})$  where

$$(\mathbf{m}^*, \mathbf{n}^*) = \operatorname{argmax}_{m, n} \sum_j A(j, m, n), \quad (6)$$

In case there are more than a single line we randomly select one.

## 5 Separable Four Points Fundamental Matrix

Given a set of putative point correspondences  $\{(x_i, x'_i)\}_{i=1 \dots N}$ , we compute the fundamental matrix by two steps. Our computation is based on RANSAC. We assume inlier ratio  $R$ , epipolar homography inlier threshold  $T_1$  and fundamental matrix inlier threshold  $T_2$ .

- **Step One.** Based on Sec. 4, we recover  $(l_{\mathbf{m}^*}, l_{\mathbf{n}^*})$ , which are the corresponding image lines with the maximum number of  $K$  putative corresponding points  $(x_i, x'_i)_{1 \dots K}$ . We select fixed control points for each line  $l_{\mathbf{m}^*}$  and  $l_{\mathbf{n}^*}$ . The points are selected on the intersection of the lines and the boundaries of the images. For each pair of putative corresponding points on the lines, we compute their representation by the control points with the two possible orientations and use the second one only if the first failed. We use RANSAC to recover the optimal three parameter model. We iteratively sample three putative corresponding points, compute the epipolar homography, transfer each point on the line to the corresponding line, and count the number of



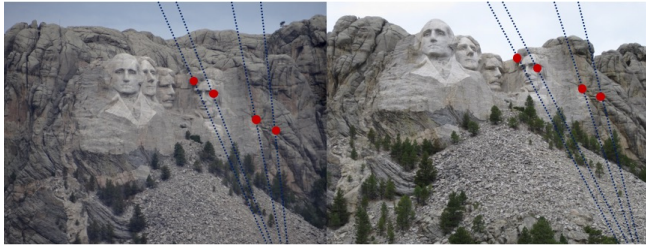


Fig. 6: Example of matched points on image line segments and corresponding epipolar lines as recovered by our approach.

inliers based on the Euclidean distance and the threshold  $T_1$ . The number of iterations is computed based on  $R$  with respect to three parameter models and is often a small number. For example, for outlier rate of 60%, we need only 71 iterations to recover the correct model with confidence of 99%. Note that although we sample three points, we require at least four corresponding points on line segment, the additional points are used for validation of the hypothesized epipolar homography.

- **Step Two.** Given the three points selected, we iteratively sample additional four points and compute the fundamental matrix based on the seven points algorithm. The number of iterations is computed based on  $R$  with respect to four parameters. We count the number of inliers based on  $T_2$  with respect to the symmetric epipolar distance [12]:

$$\sum_{i=1}^N (x'_i F x_i)^2 \left( \frac{1}{(F x_i)_1^2 + (F x_i)_2^2} + \frac{1}{(F^T x'_i)_1^2 + (F^T x'_i)_2^2} \right)$$

where  $(\cdot)_k^2$  represents the square error of the  $k$ -th entry of the vector. For the same case as above of outlier rate of 60%, for the four parameters' model we need only 178 iterations.

The above refers to the implementation of our approach based on the seven points algorithm. For implementation based on the eight points algorithm, the second step should be changed. Instead of sampling additional four points, we sample additional five points.

Figure 6 shows an example [1] of corresponding points recovered by the first step of our approach.

## 6 Experiments

### 6.1 Datasets

We conduct experiments on the following real world datasets: (1) The Strecha datasets [26] which include ground truth cameras and reconstruction, (2) The

	Pairs	Ground truth
Strecha	569	Given
Tanks and Temples	2000	COLMAP
Flickr	2000	COLMAP

Table 1: Datasets properties. For both Tanks and Temples and Flickr we obtained the ground truth fundamental matrices based on COLMAP reconstruction.

Family sequence from the Tanks and Temples dataset [15], which includes wide baseline camera poses, with medium size images captured by a hand-held camera, and (3) The Tower of London sequence from the Flickr dataset [29], where the images were downloaded from Flickr based on geotag. It represents generic cases of fundamental matrix estimation and includes images captured by the community at random camera positions over very wide baselines. Fig. 7 shows images from each of the datasets. Image pairs with matching points from the Tower of London, Family and Strecha datasets are presented in Appendix A.

For the last two datasets, we sampled 2000 image pairs with at least 20 matches with a symmetric epipolar distance of less than equal to 1 pixel with respect to the ground truth, and used them for the evaluation. We show that our approach is able to successfully compute the fundamental matrices for these real-world diverse sets of image pairs, leading to an efficient estimation process. Table 1 shows the databases properties.

## 6.2 Experiment Details

We compared RANSAC-based [10] and LMEDS-based [22] computations of the fundamental matrix based on the following minimal solvers’ methods:

- RANSAC with the standard eight points algorithm, denoted as RANSAC.
- LMEDS with the standard eight points algorithm, denoted as LMEDS.
- State-of-the-art minimal solver of [2] combined with GC-RANSAC [3], which is based on homography and rotation information of five points, denoted as Hom-Rot-5.
- RANSAC with our minimal sampling solver, using the seven points algorithm based on two samples of three and four points, denoted as Ours-RANSAC-4.



Fig. 7: Left to right, images from: (a) Tower of London from the flicker dataset (b) Family sequence from Tanks and Temples and (c) the Castle sequence from the Strecha dataset.

	% inliers	F-Score	Mean
RANSAC	71.2	$0.89 \pm 0.05$	0.61
LMEDS	71.1	$0.88 \pm 0.08$	0.59
Hom-Rot-5	71.5	$0.90 \pm 0.06$	0.60
Ours-LMEDS-4	62.4	$0.81 \pm 0.06$	0.72
Ours-LMEDS-5	72.1	$0.90 \pm 0.05$	0.59
Ours-RANSAC-4	61.7	$0.82 \pm 0.06$	0.71
Ours-RANSAC-5	<b>72.2</b>	<b><math>0.91 \pm 0.05</math></b>	<b>0.58</b>

Table 2: Results of the Strecha dataset, based on the ground truth camera poses. Our RANSAC-based eight points approach outperforms the baselines in all the metrics.

- RANSAC with our minimal sampling solver, using the eight points algorithm based on two samples of three and five points, denoted as Ours-RANSAC-5.
- LMEDS with our minimal sampling solver, using the seven points algorithm based on two samples of three and four points, denoted as Ours-LMEDS-4.
- LMEDS with our minimal sampling solver, using the eight points algorithm based on two samples of three and five points, denoted as Ours-LMEDS-5.

For the baseline methods we performed a grid-search over hyperparameters. For sequences with no ground truth fundamental matrices, we reconstructed the sequences using COLMAP [23]. COLMAP is a general purpose Structure-from-Motion (SfM) pipeline which globally infers the 3D structure, leading to accurate results. We obtained the camera poses and fundamental matrices, and used them as the ground truth.

For all sequences, we used the SIFT [17] descriptor to extract and match putative points’ correspondences between all pairs of images. We used the ground truth fundamental matrices to evaluate the symmetric epipolar distance of the putative matching. Each image pair with less than 20 matches within a symmetric epipolar distance of one is discarded.

We report the average symmetric epipolar distance resulting by our approach and the baselines. Unless otherwise stated, we used a threshold of 3 pixels in our approach as the inlier threshold and 0.35 as the epipolar homography threshold. We use a fixed homography threshold over all the datasets, demonstrating its robustness.

We report the percentage of inliers found by each method, and report the F-measure, where corresponding points with symmetric epipolar distance less than 1 pixel with respect to the ground truth fundamental matrix is considered as positive.

### 6.3 Accuracy

**Strecha.** The dataset contains eight multi-view collections of high-resolution images ( $3072 \times 2048$ ), provided with ground truth camera poses. For the computation of matching lines with putative corresponding points across images, we

	% inliers	F-Score	Mean
RANSAC	45.4	<b>0.72 <math>\pm</math> 0.07</b>	0.69
LMEDS	44.2	0.71 $\pm$ 0.08	0.68
Hom-Rot-5	45.5	<b>0.72 <math>\pm</math> 0.07</b>	<b>0.61</b>
Ours-LMEDS-4	43.8	0.61 $\pm$ 0.09	0.66
Ours-LMEDS-5	45.7	0.71 $\pm$ 0.07	0.11
Ours-RANSAC-4	44	0.62 $\pm$ 0.08	0.13
Ours-RANSAC-5	<b>48.1</b>	<b>0.72 <math>\pm</math> 0.07</b>	0.63

Table 3: Results on the Family sequence from the Tanks and Temples dataset. Our RANSAC-based eight points approach and the approach of [2] are comparable, and perform better than other methods.

	% inliers	F-Score	Mean
RANSAC	43.7	0.52 $\pm$ 0.08	0.63
LMEDS	43.2	0.53 $\pm$ 0.09	0.69
Hom-Rot-5	44.5	0.58 $\pm$ 0.08	0.61
Ours-LMEDS-4	41.6	0.51 $\pm$ 0.1	0.74
Ours-LMEDS-5	46.5	0.60 $\pm$ 0.09	0.57
Ours-RANSAC-4	42.9	0.51 $\pm$ 0.1	0.78
Ours-RANSAC-5	<b>49.3</b>	<b>0.62 <math>\pm</math> 0.09</b>	<b>0.54</b>

Table 4: Results on Tower of London sequence from the Flickr dataset. Our RANSAC-based eight points approach performs better, with a clear margin, than all other methods.

sample 150 putative correspondences, and used these lines with respect to all existing points’ correspondences. We used SIFT ratio-test of 0.75. The binary images used for matching the lines (Sec. 4) are of a lower resolution, as suggested in [27,28], and the points coordinates are resized accordingly. Unless noted otherwise, the width resolution of 1024 was used for the line matching phase with the original aspect ratio. The reported results are with respect to the original resolutions. The sequences are of images with varying distances between focal points with overall of 569 valid image pairs. As suggested in [2], we used the five-points’ solver of [2] within the GC-RANSAC [3] estimator. Table. 2 presents our result. In all metrics our RANSAC-based eight points approach outperforms the baselines.

**Tanks and Temples.** The dataset includes medium-resolution images ( $1920 \times 1080$ ). For comparisons, we used the Family sequence. As ground truth, we use the COLMAP Reconstruction. As shown in Table 3, our RANSAC-based eight points approach performs similarly to [2], and both outperform other methods.

	RANSAC Iterations	%Failure
RANSAC	2931	<b>0.2</b>
Hom-Rot-5	671	5.2
Ours-LMEDS-4	<b>621</b>	7.8
Ours-LMEDS-5	639	4.3
Ours-RANSAC-4	<b>621</b>	7.4
Ours-RANSAC-5	639	3.9
Ours-EXT-RANSAC-5	732	0.3

Table 5: The number of RANSAC iterations and failure cases for all three datasets. Both our Median-based and RANSAC-based eight points require less iterations with lower failure cases than the baseline approach. RANSAC presents the lower failure rate and the higher number of iterations. Ours-EXT-RANSAC-5 presents the most cost-effective solution, see text for details.

**Flickr.** The dataset contains medium to large-scale internet datasets obtained by downloading images of specific scenes from Flickr. The images captured by random people at different times, with various cameras from very different positions. We use the Tower of London sequence for comparison. We reconstruct the sequence using COLMAP[23] and use the reconstruction as ground truth. The results are presented in Table 3, where it can be seen that our RANSAC-based eight points approach clearly outperforms all other methods.

## 6.4 Efficiency

We measured the number of RANSAC iterations required by each method and the number of failure cases. For the total number of RANSAC iterations, we also consider all validation iterations. For methods which are based on the seven points algorithm, both ours and the baseline, there might be more iterations than the theoretical number of required samples. A failure is considered if the solver has not been able to accurately recover at least 20 matches, in case there are indeed such ground truth matches.

The solver of [2] is combined within another robust estimator framework, the GC-RANSAC [3]. We execute only the solver itself with the optimal number of iterations as an initialization. In both methods, ours and [2], we used the cardinality of the best inliers set found so far in each iterations to estimate the maximum required number of samples. Our approach starts by finding the matching lines with the maximum number of putative correspondences (Sec. 5). In case the inlier ratio is known to be less than 30%, we use instead the standard RANSAC to reduce the additional overhead associated with this step. The runtime of our matching step is equivalent to 59 RANSAC iterations, and each pair of images was measured and added to the overall number of required samples by our approach. In this experiment we tested an additional method, denoted as Ours-EXT-RANSAC-5. This method is the same as Ours-RANSAC-5 but switches to standard RANSAC in case we can not recover matching lines after

sampling the first four points, thus significantly reducing the number of failure cases while adding only a small number of iterations.

Table 5 shows the percentage of cases that failed for each approach and the average number of iterations, over all the three datasets, the Strecha, Tanks and Temples and Flickr. Our approach has been able to successfully compute the fundamental matrices for more cases in fewer iterations. Using the seven points algorithm, our approach requires less iterations but is less robust.

## 7 Discussion

**Robustness.** Typically, in an urban scene there are several hundred lines candidates with at least four correspondences and several dozen corresponding lines with accurate epipolar homography. The average number of candidate lines in the Strecha dataset is 312.4 and the average points on matched lines is 7.6 with a maximum of 23. A successful line matching is mainly related to the density of feature points in the images and the required accuracy of the epipolar line homography. We resize the images to a width of 1024 pixels and use a threshold of 0.35 for the epipolar homography. We found that these parameters performed well and it is the recommended starting point. Resizing the images to 512 and setting the threshold up to 1 pixel, our method still performs well. We observed that our approach can perform well in low inlier cases when the absolute number of inliers is higher than a given amount. We therefore recommend at least 150 inliers for such scenarios, which is often the case in our datasets.

**Failure Cases.** A typical failure case is in a very wide baseline where the matching accuracy of feature points is not sufficient. During the evaluation of the epipolar line homography we consider the deviations of the correspondences from the computed line as too large and reject it. Manually increasing the threshold successfully recovers the line. An additional typical failure case is where there is only a small number of inliers, typically fewer than 60. Often in this case the deviation of the feature points from candidate lines is too large due to their spread in the image and our homography computation fails.

## 8 Conclusion

We presented an approach for the computation of the fundamental matrix based on epipolar homography decomposition. Our approach can reduce, both theoretically and practically, the number of required evaluation iterations to a new minimal number. We have shown empirically that our approach is accurate and that it consistently expedites the computation process. The standard RANSAC procedure can be incorporated into our approach, providing an overall robust and efficient solution which is well suited for Structure from Motion (SfM) pipelines.

## References

1. Mount rushmore, <https://www.cc.gatech.edu/~hays/compvision/>
2. Barath, D.: Five-point fundamental matrix estimation for uncalibrated cameras. In: Proceedings of the IEEE Conference on Computer Vision and Pattern Recognition. pp. 235–243 (2018)
3. Barath, D., Matas, J.: Graph-cut ransac. In: Proceedings of the IEEE Conference on Computer Vision and Pattern Recognition. pp. 6733–6741 (2018)
4. Barath, D., Matas, J., Nuskova, J.: Magsac: marginalizing sample consensus. In: Proceedings of the IEEE Conference on Computer Vision and Pattern Recognition. pp. 10197–10205 (2019)
5. Ben-Artzi, G., Halperin, T., Werman, M., Peleg, S.: Epipolar geometry based on line similarity. In: 2016 23rd International Conference on Pattern Recognition (ICPR). pp. 1864–1869. IEEE (2016)
6. Ben-Artzi, G., Kasten, Y., Peleg, S., Werman, M.: Camera calibration from dynamic silhouettes using motion barcodes. In: Proceedings of the IEEE Conference on Computer Vision and Pattern Recognition. pp. 4095–4103 (2016)
7. Chum, O., Matas, J.: Matching with prosac-progressive sample consensus. In: 2005 IEEE computer society conference on computer vision and pattern recognition (CVPR'05). vol. 1, pp. 220–226. IEEE (2005)
8. Duda, R.O., Hart, P.E.: Use of the hough transformation to detect lines and curves in pictures. Tech. rep., Sri International Menlo Park Ca Artificial Intelligence Center (1971)
9. Faugeras, O., Luong, Q.T., Papadopoulos, T.: The geometry of multiple images: the laws that govern the formation of multiple images of a scene and some of their applications. MIT press (2001)
10. Fischler, M.A., Bolles, R.C.: Random sample consensus: A paradigm for model fitting with applications to image analysis and automated cartography. Commun. ACM **24**(6), 381–395 (Jun 1981). <https://doi.org/10.1145/358669.358692>, <http://doi.acm.org/10.1145/358669.358692>
11. Halperin, T., Werman, M.: An epipolar line from a single pixel. In: 2018 IEEE Winter Conference on Applications of Computer Vision (WACV). pp. 983–991. IEEE (2018)
12. Hartley, R., Zisserman, A.: Multiple view geometry in computer vision. Cambridge university press (2003)
13. Hartley, R.I.: In defense of the eight-point algorithm. Pattern Analysis and Machine Intelligence, IEEE Transactions on **19**(6), 580–593 (1997)
14. Kasten, Y., Ben-Artzi, G., Peleg, S., Werman, M.: Fundamental matrices from moving objects using line motion barcodes. In: European Conference on Computer Vision. pp. 220–228. Springer (2016)
15. Knapitsch, A., Park, J., Zhou, Q.Y., Koltun, V.: Tanks and temples: Benchmarking large-scale scene reconstruction. ACM Transactions on Graphics **36**(4) (2017)
16. Longuet-Higgins, H.C.: A computer algorithm for reconstructing a scene from two projections. Readings in Computer Vision: Issues, Problems, Principles, and Paradigms, MA Fischler and O. Firschein, eds pp. 61–62 (1987)
17. Lowe, D.G.: Distinctive image features from scale-invariant keypoints. International journal of computer vision **60**(2), 91–110 (2004)
18. Luong, Q.T., Faugeras, O.D.: The fundamental matrix: Theory, algorithms, and stability analysis. International journal of computer vision **17**(1), 43–75 (1996)

19. Nistér, D.: An efficient solution to the five-point relative pose problem. *IEEE transactions on pattern analysis and machine intelligence* **26**(6), 0756–777 (2004)
20. Nistér, D.: Preemptive ransac for live structure and motion estimation. *Machine Vision and Applications* **16**(5), 321–329 (2005)
21. Reisner-Kollmann, I., Reichinger, A., Purgathofer, W.: 3d camera pose estimation using line correspondences and 1d homographies. In: *International Symposium on Visual Computing*. pp. 41–52. Springer (2010)
22. Rousseeuw, P.J.: Least median of squares regression. *Journal of the American statistical association* **79**(388), 871–880 (1984)
23. Schönberger, J.L., Frahm, J.M.: Structure-from-motion revisited. In: *Conference on Computer Vision and Pattern Recognition (CVPR)* (2016)
24. Sinha, S.N., Pollefeys, M.: Camera network calibration and synchronization from silhouettes in archived video. *International journal of computer vision* **87**(3), 266–283 (2010)
25. Stewénius, H., Nistér, D., Kahl, F., Schaffalitzky, F.: A minimal solution for relative pose with unknown focal length. In: *2005 IEEE Computer Society Conference on Computer Vision and Pattern Recognition (CVPR’05)*. vol. 2, pp. 789–794. IEEE (2005)
26. Strecha, C., Von Hansen, W., Van Gool, L., Fua, P., Thoennessen, U.: On benchmarking camera calibration and multi-view stereo for high resolution imagery. In: *2008 IEEE Conference on Computer Vision and Pattern Recognition*. pp. 1–8. Ieee (2008)
27. Tola, E., Lepetit, V., Fua, P.: Daisy: An efficient dense descriptor applied to wide-baseline stereo. *IEEE transactions on pattern analysis and machine intelligence* **32**(5), 815–830 (2009)
28. Trulls, E., Kokkinos, I., Sanfeliu, A., Moreno-Noguer, F.: Dense segmentation-aware descriptors. In: *Proceedings of the IEEE Conference on Computer Vision and Pattern Recognition*. pp. 2890–2897 (2013)
29. Wilson, K., Snavely, N.: Robust global translations with 1dsfm. In: *European Conference on Computer Vision*. pp. 61–75. Springer (2014)
30. Wurfl, T., Aichert, A., Maass, N., Dennerlein, F., Maier, A.: Estimating the fundamental matrix without point correspondences with application to transmission imaging. In: *Proceedings of the IEEE International Conference on Computer Vision*. pp. 1072–1081 (2019)



## A Appendix

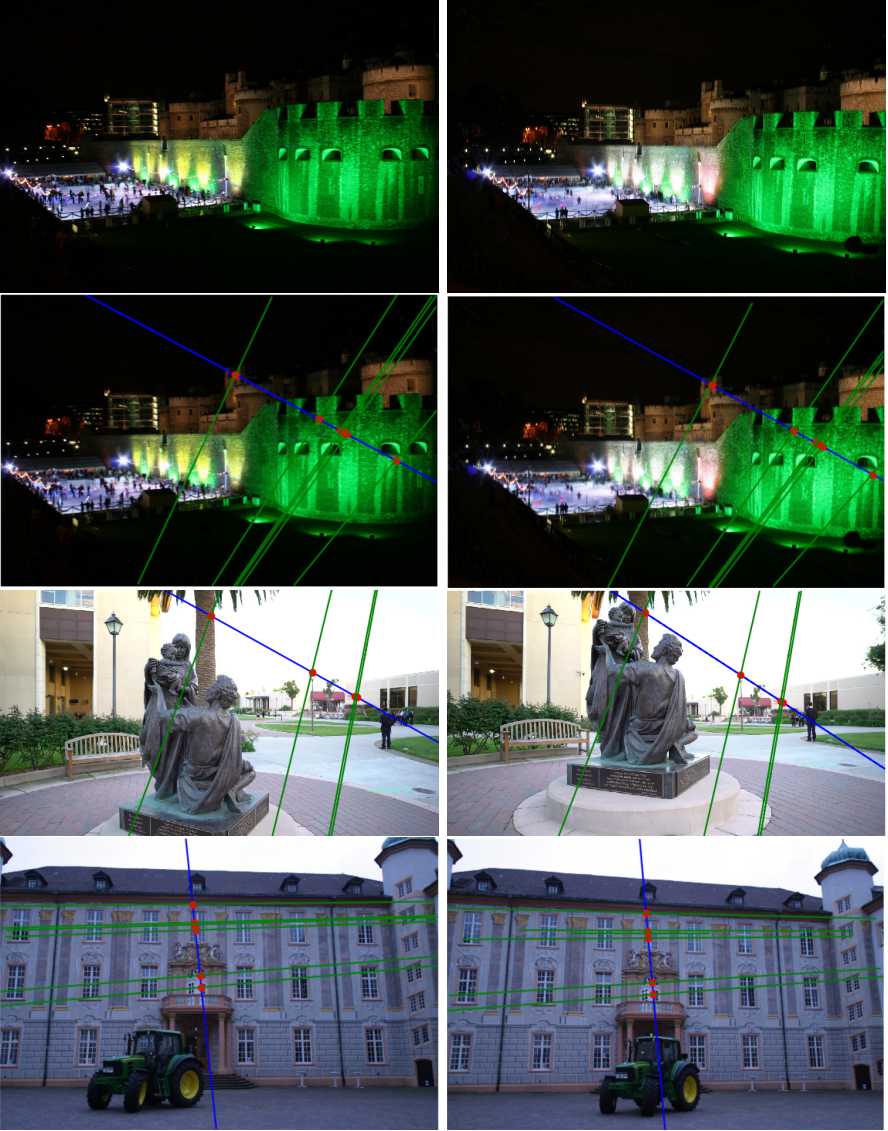


Image pairs with matching points on lines segments from the datasets. Top to bottom rows: Tower of London (Flickr) without (first row) and with (second row) matched points, Family sequence (Tanks and Temples) and the Castle sequence (Strecha). Red points are the matches and green lines are epipolar lines.